Title Page (with Author Details)

Multimodal and multiscale non-invasive study of Leonardo's Mural Painting in *Sala delle Asse* (Milan): a tool supporting cleaning evaluation

Alessandra Botteon[a*], Claudia Conti[a], Chiara Colombo[a], Maria Catrambone[a], Marco Realini[a], Costanza Miliani[b], Sotiria Kogou[c], Sammy Cheung[c], Haida Liang[c], Francesca Tasso[d], Michela Palazzo[e], and Antonio Sansonetti[a]

[a] *Institute of Heritage Science, National Research Council (CNR ISPC), Via R. Cozzi 53, 20125 Milan, Italy*

[b] *Institute of Heritage Science, National Research Council (CNR ISPC), Via Card. G. Sanfelice, 8, 80134, Naples, Italy*

[c] *ISAAC Laboratory, School of Science and Technology, Nottingham Trent University, Nottingham, NG11 8NS UK*

[d] Comune di Milano, Musei del Castello Sforzesco, Archeologici e Museo del Risorgimento, Comune di Milano, Piazza Duomo 14, 20122, Milano, Italy

[e] Direzione Regionale Musei Nazionali Lombardia, Ministero della Cultura, Corso Magenta 24, 20123, Milano, Italy

*Corresponding author: alessandra.botteon@cnr.it

Length of the manuscript: the exact number of words of the manuscript is 5802, including tables and references; 4406 words excluding tables and references.

Multimodal and multiscale non-invasive study of Leonardo's Mural Painting in *Sala delle Asse* (Milan): a tool supporting cleaning evaluation

Alessandra Botteon[a*], Claudia Conti[a], Chiara Colombo[a], Maria Catrambone[a], Marco Realini[a], Costanza Miliani[b], Sotiria Kogou[c], Sammy Cheung[c], Haida Liang[c], Francesca Tasso[d], Michela Palazzo[e], and Antonio Sansonetti[a]

[a] *Institute of Heritage Science, National Research Council (CNR ISPC), Via R. Cozzi 53, 20125 Milan, Italy*

[b] *Institute of Heritage Science, National Research Council (CNR ISPC), Via Card. G. Sanfelice, 8, 80134, Naples, Italy*

[c] *ISAAC Laboratory, School of Science and Technology, Nottingham Trent University, Nottingham, NG11 8NS UK*

[d] Comune di Milano, Musei del Castello Sforzesco, Archeologici e Museo del Risorgimento, Piazza Duomo 14, 20122, Milano, Italy

[e] Direzione Regionale Musei Nazionali Lombardia, Ministero della Cultura, Corso Magenta 24, 20123, Milano, Italy

*Corresponding author: alessandra.botteon@cnr.it

Abstract

Sala delle Asse in the Milan Sforza Castle was decorated by Leonardo da Vinci and his workshop at the end of the XV century. Due to historical events involving the Duchy of Milan, the decoration of the room was interrupted in 1499 and some areas remained devoid of polychrome paintings. For this reason, the painted surfaces were whitewashed and forgotten for a long-time, but during the 19th and 20th centuries, they were rediscovered and restored twice, uncovering the remnants of original layers.

In recent years, the hall has been the focus of a comprehensive project aimed at thoroughly assessing the conservation issues of its walls and optimizing the necessary intervention methods. One of the primary objectives of this project is to restore the legibility of the original painting remnants. For this purpose, cleaning tests have been conducted with different methodologies on specific sections of the walls.

This study employs a multimodal and multiscale approach conducted in situ on both cleaned and uncleaned polychrome areas of the walls to provide an overview of the pigments used by Leonardo da Vinci and his workshop. Additionally, it evaluates the effectiveness of cleaning procedures in removing 19th and 20th century overpainting, thereby revealing the underlying painted layers.

The non-invasive approach includes portable micro- X-Ray Fluorescence (point-based measurements and micro-mapping), portable Raman spectroscopy (point measurements and micro-spatially offset Raman spectroscopy), and mobile remote standoff spectral imaging, carried out at a stand-off distance of ~ 10m. The integration of imaging and point-based data collected at remote and close distance, with centimetre scale field of view and sub-millimetres spatial resolution (remote standoff imaging) and millimetres and

micrometres spot size (point measurements), provided valuable insights on elemental and molecular composition of the materials present both in the uncleaned and cleaned areas of the mural painting, permitting a partial reconstruction of the stratigraphy and thus shedding light on the 15th century paint residues; moreover, the study expands the up-to-date protocols for the non-invasive identification of pigments and for an integrated evaluation of cleaning effectiveness.

Keywords: remote spectral imaging; micro-SORS; micro-XRF mapping; Leonardo da Vinci; mural painting.

1. INTRODUCTION AND RESEARCH AIM

Sala delle Asse is a renowned hall in the *Falconiera* Tower in Milan Sforza Castle; at the seat of Duke Ludovico il Moro, at the end of the XV century, the painted decoration of the walls and the vault was entrusted to Leonardo da Vinci and his workshop. The walls and the vault of the room were planned to be covered with paintings representing interlaced branches, gilt ropes, and coat of arms reporting some mottoes; the painted decoration was never finished due to Ludovico's fall. Painted surfaces were whitewashed and forgotten for a long-time but during the 19th and 20th centuries, they were rediscovered, and works was carried out for uncovering the remnants of original layers [1,2]. Currently the vault is still covered by polychrome layers of repaintings depicting an arbour, while on the walls, where there is no polychrome painting, several portions of drawings of landscapes are conserved, amongst which is the so called "Monochrome" universally attributed to Leonardo himself.

The conservation challenge arises by the history of the wall paintings, which were rediscovered due to the mechanical removal of the whitewash during the refurbishment of the Sforza Castle, in the last decade of the 19th century, to adapt it to the new Museum uses. Then in the first decades of the 20th century the remnants of the paintings were heavily integrated, reshaping them under the influence of "arts and crafts" triumphant style; those repaintings were considered too invasive during the 1954-1956 intervention, hence the painted surfaces were modified with brushing and sponging; currently it could be estimated that ancients painting layers are only a small percentage of the visible pattern. This previous conservation history makes the surface composition heterogeneous: the painted surface appears with decay products, whitewash remnants, and glue residues, probably due to the attempt to even out the painted surface during the last conservation works in the 50's.

To develop the conservation best practice, an in-depth study of the materials applied on the room surfaces is in progress. Starting from 2013, a complex project was planned to study the conservation issues, and to optimize the intervention methods; among these, multipurpose cleaning actions were tested to allow a correct reading of the painting remnants. For this purpose, cleaning trials have been carried out, both with laser and with gel cleaning, searching for the best effect in removal of whitewash, overpaintings and soluble salt formations.

Hence, cleaned and uncleaned areas were close to each other in selected portions of the mural painting and a scaffolding was setup for access to the large walls (the room measures 15 meters on each side and 10 meters in height).

Here we present a multimodal non-invasive and in-situ approach focused on obtaining an overview of the original pigments used in 15th century by Leonardo and his workshop, through analysis of the cleaned area where the successive overpaintings and other non-original substances were cleaned off. Despite the small residues of 15th century painting in a very severe conservation state, the information that can be achieved non-invasively are particularly relevant to expand the existing scientific literature about Leonardo's mural painting techniques and palette [3–11].

Moreover, the characterization of the materials used in the modern restoration actions, which can be obtained analysing the uncleaned areas, would allow an identification of possible residues of the modern materials in the cleaned area, permitting an evaluation of the degree of the cleaning procedures in unveiling underneath, 15th century painting layers. This approach is to be considered, encompassing it in a methodological point of view, as part of a complex analytical protocol aimed at the evaluation of the cleaning operations.

The analytical protocol includes mobile remote large-scale spectral imaging, carried out at a stand-off distance of approximately 10 meters, complemented by close-distance analysis, such as portable X-Ray Fluorescence (pXRF) for point measurements and micro-mapping, alongside portable Raman spectroscopy (pRaman) employing both conventional and micro-spatially offset Raman spectroscopy. The close-distance measurements, facilitated by scaffolding, presents challenges, such as potential vibrations during acquisition and space constraints due to the presence of instrumental tripods and scaffolding. Conversely, ground-based remote standoff spectral imaging allows for high spatial resolution and large-scale examination of otherwise inaccessible areas, such as the vault, from stable ground. The complementarity between large-scale spectral imaging and close-distance analysis lies in the ability to use data from Raman and XRF spectroscopy to more accurately interpret reflectance spectra, whose complexity reflects that of the materials present on the walls of the *Sala*.

Following this approach, we provided an in-depth elemental and molecular compositional characterization of the substances present both in the uncleaned and cleaned areas of the mural painting. In the last decades, numerous efforts were made for characterising mural paintings, rock art and street art paintings in situ and in a non-invasive way [12–23]. This study enriches the state of the art, offering an unusual and effective synergy between conventional and advanced remote imaging in a renowned scenario such as the one in *Sala delle Asse*.

Moreover, the analytical protocol proposed is considered a fruitful tool in evaluating cleaning procedure in the special case when removal of overpainting is involved, so that the analytical maps obtained can provide information about the cleaning effectiveness, its level of completion, the remnants of overpainting. The protocol raises from the combination of both remote and close distance analytical data.

2. METHODS

The investigated area includes uncleaned painted surface and three adjacent cleaning tests on the north-west wall of the room (Fig. 1).

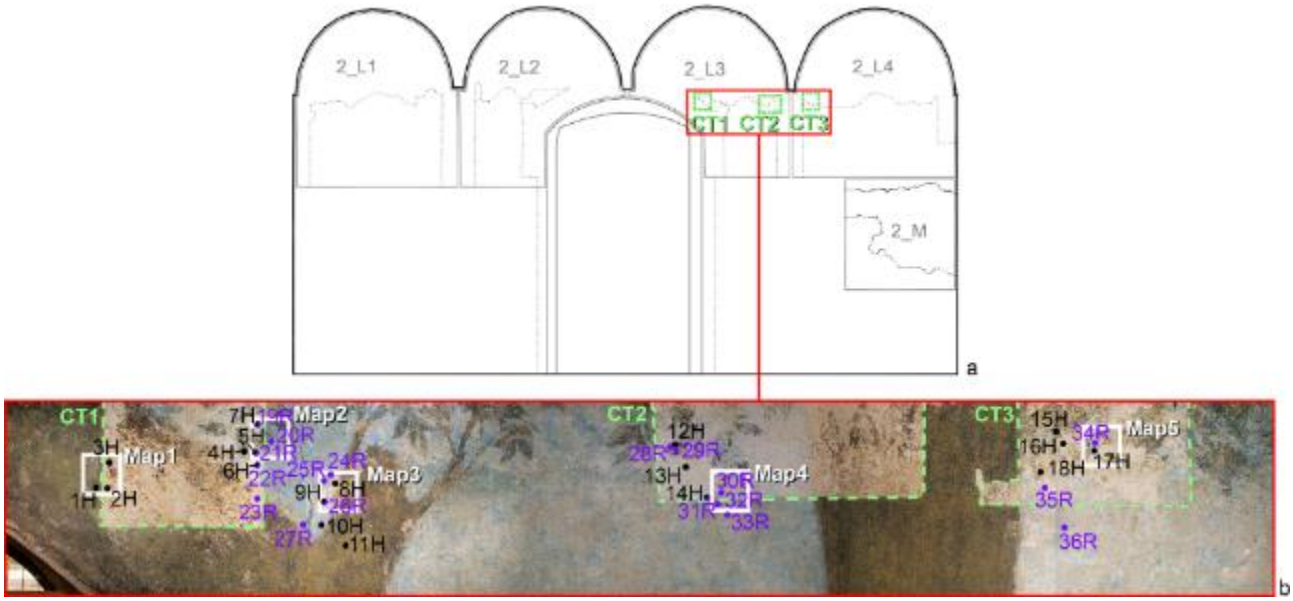

Fig. 1 (a) Scheme of the north-west wall with indication of the analysed area (red rectangle) and the location of the three cleaning tests (CT1-3); (b) digital reconstruction of analysed area with indication of cleaning tests (CT1-3), XRF point measurements (1H-18H), Raman measurements (19R-36R) and XRF maps (Map1-Map5); the digital reconstruction was obtained merging several pictures of the wall. The original pictures can be found in the supplementary material (Figure S1).

The large-scale spectral imaging of the wall paintings was performed from a stand-off distance of ~ 10m using a mobile spectral imaging system PRISMS [20], developed by the ISAAC group. It is a filter-based system, with 10 filters (from 400nm to 850nm with spacing of 50nm). The angular spatial resolution is 39 µrad (i.e. 0.39 mm at 10 m distance) for this large-scale survey setup, while the spectral bandwidth of the filters is 40 nm. The pixel-level spectra acquired with spectral imaging are clustered into groups with similar spectra using a machine learning method developed by the ISAAC group [21].

Fig. 2 Non-invasive measurements on the painted walls of the room; ground-based spectral imaging has been performed remotely, XRF and Raman spectroscopy closely to the walls on the scaffolding.

XRF spectroscopy was carried out with a portable XRF analyser (pXRF) Elio (Bruker) composed by an excitation Rh target X-ray tube, 10 kV – 50 kV, 5 µA – 200 µA, 4 W, a SDD detector (area 17 mm²) with CUBE

technology, energy resolution < 140 eV for Mn Kα, and collimator of 1 mm. The detected elements range from Mg (Z = 12) (with helium purge) to U (Z = 92). The instrument is equipped with two pointing lasers (axial and focal) for the alignment and with an internal digital camera to acquire a magnified image of the analysed area, with a field of view 10 mm x 10 mm. The analyser is fixed on a motorized XY stage, in turn mounted on a tripod (height 43-188cm) for 2D mapping with a travel range of 100 mm x 100 mm. The dimensions of measurement head are 170 mm x 265 mm x 170 mm (W x D x H), the weight 2.1 kg. The data acquisition is controlled by software package ELIO, the post processing mapping analysis is performed by ESPRIT Reveal software. Both point measurements and maps were performed. Point measurements were collected with an acquisition time of 140s; areas of 90 × 90 mm^2 were mapped with 1 mm steps size and an acquisition time of 1s per pixel; parameters of the x-ray tube were 80 μA and 40 kV.

Raman measurements were carried out with a portable Xantus-2™ Raman spectrometer (Rigaku, Boston, USA), equipped with a thermoelectrically cooled CCD and two excitation wavelengths, namely 785 nm and 1064 nm. The instrument is modified for performing the defocusing micro-SORS analysis[24], a method that allows to retrieve non-invasively the subsurface composition of stratified, turbid materials directly from the surface [25]. Defocused micro-SORS spectra were collected by moving the instrument away from the paintings, starting from the surface in focus position up to 600 μm of defocusing distance, with defocusing steps of 100 μm. Both conventional and micro-SORS spectra were acquired using a laser power ranging between 50 and 100 mW, and an acquisition time ranging between 5s to 20s.

3. RESULTS AND DISCUSSION

The results of the clustering of reflectance spectra are presented via false colour maps, facilitating a comprehensive depiction of compound distribution across wall paintings at a macroscopic level.

Fig. 3 shows the overall cluster maps related to cleaned areas CT1 and CT2 and to part of the uncleaned area between them. Significantly, the analysis underscores unequivocal compositional disparities between cleaned and uncleaned regions, indicating substantial removal of pictorial layers related to overpainting during the cleaning process. In the uncleaned areas (Fig 3e, f) three primary clusters were identified, the first associated to tree trunks, branches, and leaves (green in the false colour cluster map), the second and the third associated to the sky (red and purple in the false colour cluster map). In the cleaned areas two main cluster are observed (light green and beige in the false colour cluster map).

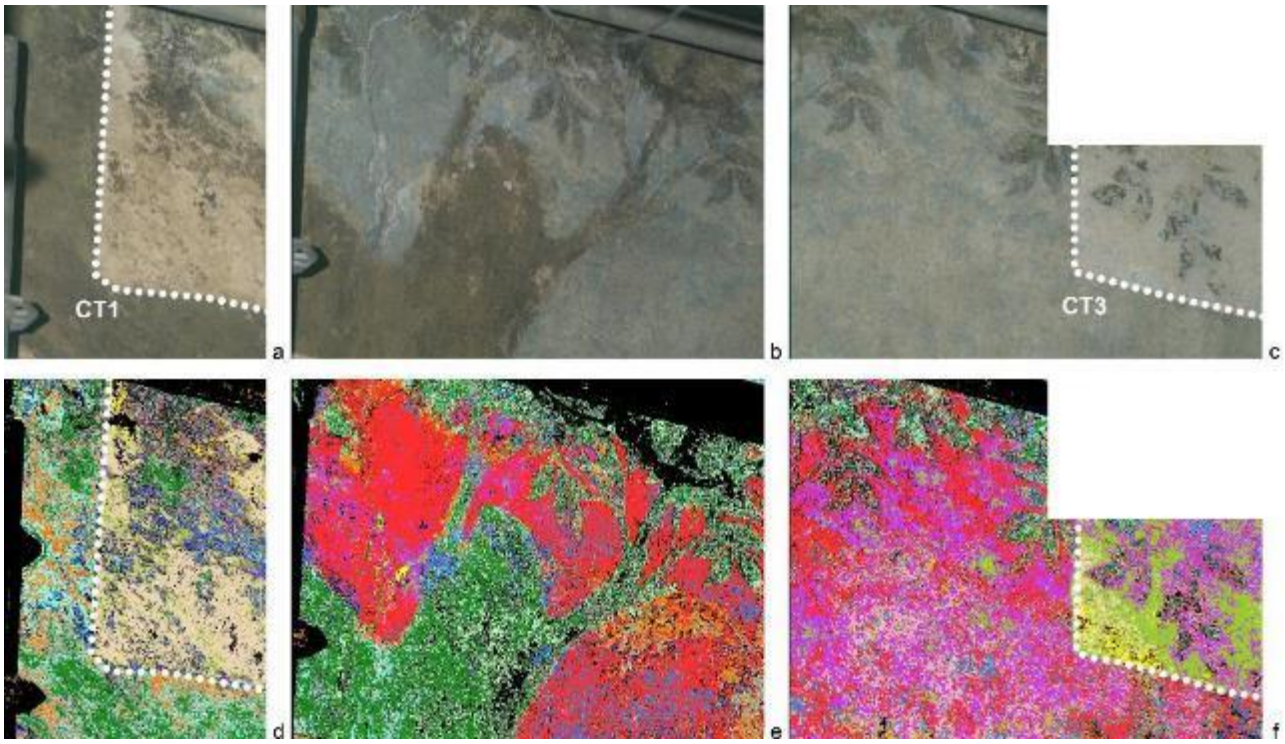

Fig. 3 (a-c) RGB images derived from PRISMS system; (d-f) Overall cluster maps. The white dashed boxes indicate the cleaned areas CT1 and CT2.

Observation of the overall cluster maps allows the selection of smaller-scale areas with significant material variation, where micro-XRF mapping should be conducted. The pronounced reflectance spectral difference between cleaned and uncleaned sections, prompted a focused micro-XRF mapping effort at the interface of these regions. Notably, this analysis confirmed a meaningful difference in elemental distribution between cleaned and uncleaned sections and provided relevant indications about the marker elements of both recent palette and more ancient layers.

Barium, zinc, chromium, and manganese are primarily distributed within the uncleaned areas. These can be assigned to the more external and recent portion of the stratigraphy, as confirmed by their presence in specific pigments in the 19 th and 20 th centuries, such as barium white, zinc white and lithopone, and chrome-based greens as chrome green and viridian green. It is important to highlight that traces of barium, zinc, manganese and chromium are also present on the cleaned parts, suggesting the presence of residues of modern pigments (Fig. 4-6). In Map 1 and Map 4 (Fig. 4-5), lead and copper are spread on the light blue areas of the sky and on the green leaves of the cleaned part, that can be associated with the more ancient painted layers. In Map 2, lead and copper distribution on both cleaned and uncleaned areas could indicate that, in the uncleaned portion, these elements are emerging from the inner layers (Fig. 6). Nonetheless, the presence of lead-based and copper-based pigments also in the recent painted layers cannot be excluded.

Calcium distribution in Map 1 (Fig. 4) and Map 4 (Fig. 5) follows the whitish parts visible on the cleaned area, suggesting the presence of a lime-based whitewash present under the modern paint. However, the contribution of the plaster substrate to the calcium distribution cannot be excluded. Additionally, iron cannot be used as marker element since it has been detected in both areas.

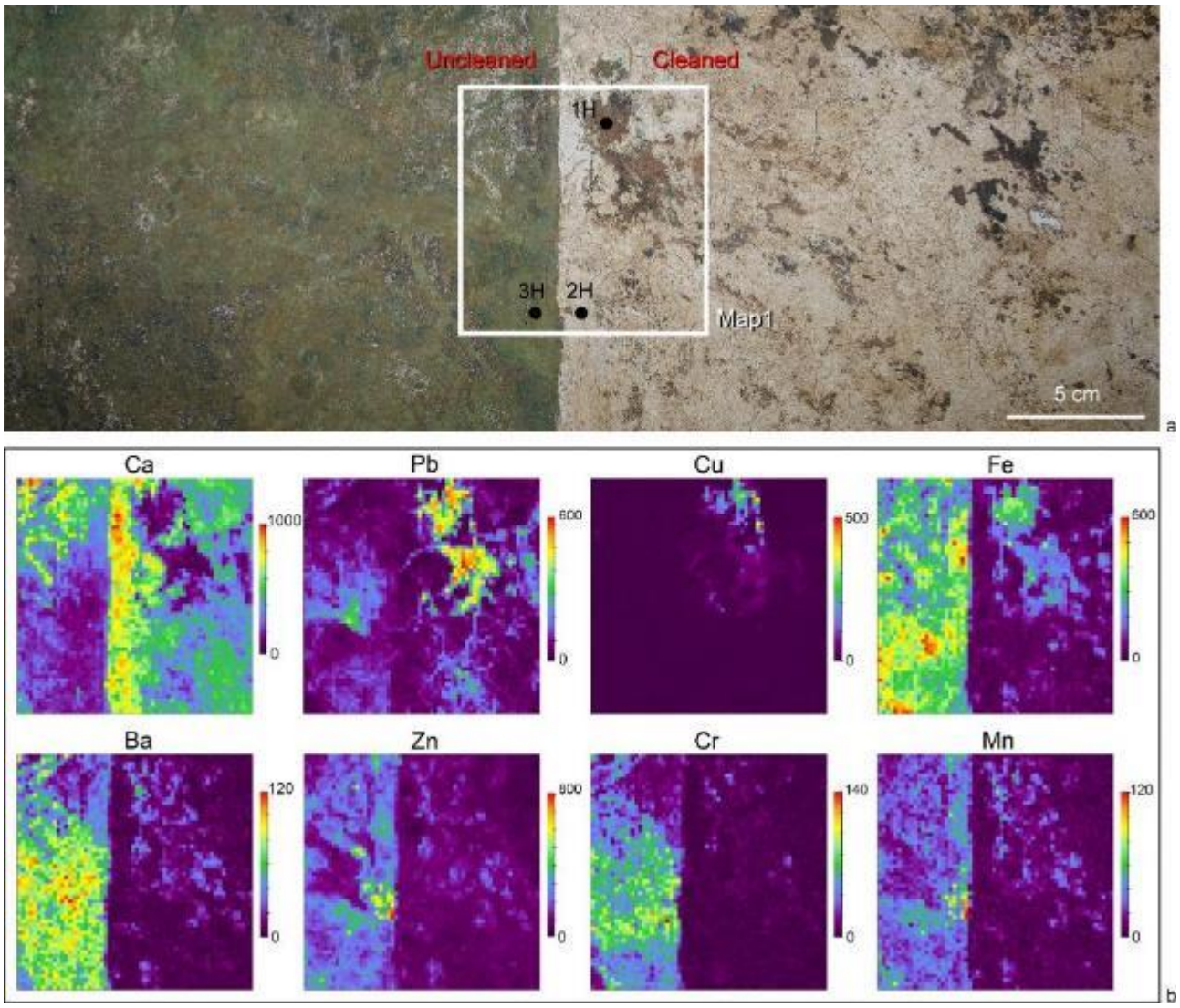

Fig. 4: Detail of an investigated area with indication of XRF Map1 location (in between an uncleaned area and CT1) and XRF point measurements H1-H3 (a); XRF elemental distribution, colour scale: cps (b).

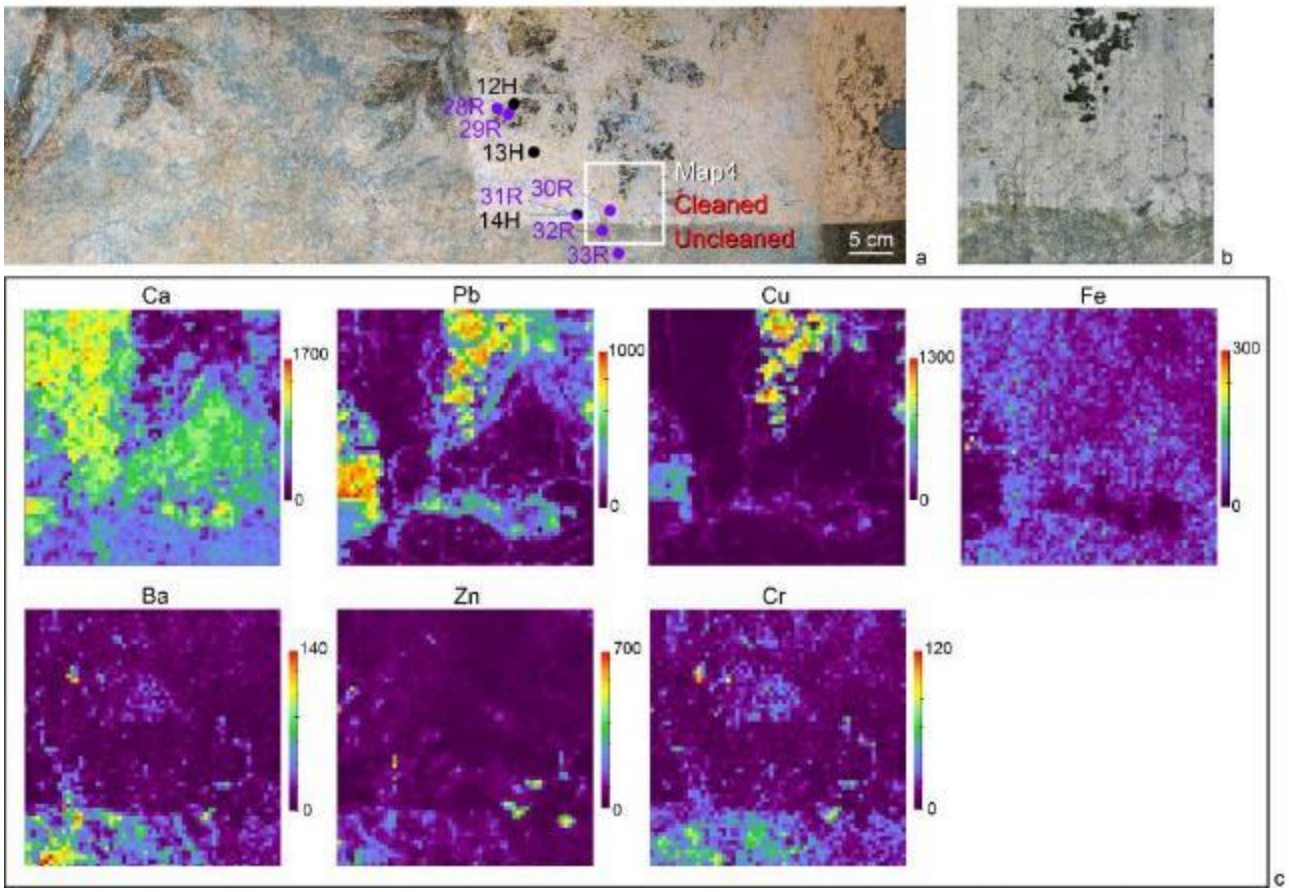

Fig. 5: Detail of an investigated area with indication of XRF Map4 location (in between an uncleaned area and CT2), XRF point measurements H12-H13 and Raman point measurements R28-R33 (a); close-up image of Map4 (b) and XRF elemental distribution, colour scale: cps (c).

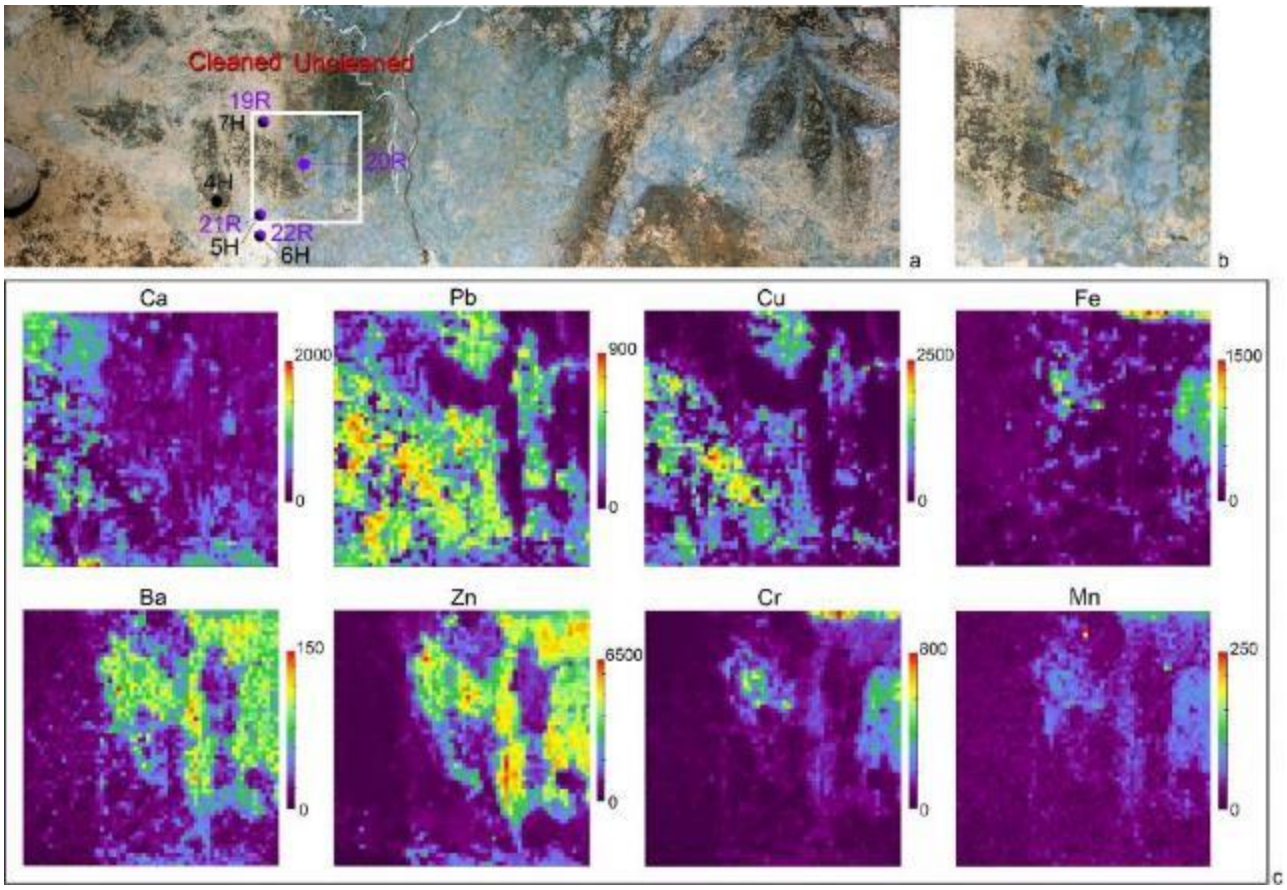

Fig. 6. Detail of an investigated area with indication of XRF Map2 location (in between an uncleaned area and CT1), XRF point measurements H4-H6 and Raman point measurements R19-R22 (a); close-up image of Map4 (b) and XRF elemental distribution, colour scale: cps (c).

For more detailed material characterisation, point XRF and Raman spectroscopies were applied to specific areas indicated by the imaging datasets.

It is worth noting that point XRF analyses offer a more detailed investigation of the chemical composition compared to micro-XRF maps. This is because point measurements, with their longer acquisition time (140 seconds for the point measurements versus 1 second per spectrum in the maps), are capable of detecting elements present in lower concentrations. In contrast, the shorter integration time required for mapping is necessary to avoid excessively long acquisition, which would otherwise make the mapping process impractically slow.

Raman spectroscopy measurements provide molecular information, and when microscope objectives are used for delivering the laser and collecting the Raman signal, they allow for the acquisition of data with high spatial resolution. The selection of the analysis has been driven by the attempt to optimize the results according to the characteristics of the techniques. For instance, a very intense fluorescence was observed in preliminary Raman spectra collected on the green areas. For this reason, green points have been mainly analysed with pXRF.

In Table 1, the summary of the outcomes of point XRF and Raman measurements is reported respectively.

Table 1. Point XRF and Raman spectroscopy measurements.

Label	**Technique**	**Detected Elements (in Z order) or Compounds**
1H (green, uncleaned)	XRF	Ca, Cr, Mn, Fe, Zn, Sn, Sb, Ba, Pb
2H (white, cleaned):	XRF	Ca, Mn, Fe, Zn, Sn, Ba, Pb
3H (brown, cleaned):	XRF	Ca, Cr, Mn, Fe, Cu, Zn, Sn, Ba, Pb

4H (brown, cleaned):	XRF	Ca, Cr, Fe, Cu, Ba, Pb
5H (blue, cleaned):	XRF	Ca, Cr, Mn, Fe, Cu, Zn, Sn, Ba, Pb
6H (whitewash, cleaned):	XRF	Ca, Fe, Cu, Sn, Pb
7H (white, cleaned):	XRF	Ca, Mn, Fe, Cu, Zn, Sn, Pb
8H (white, uncleaned):	XRF	Ca, Cr, Fe, Cu, Zn, Sn, Ba, Pb
9H (blue, uncleaned)	XRF	Ca, Cr, Mn, Fe, Cu, Zn, Sn, Ba, Pb
10H (blue, uncleaned)	XRF	Ca, Cr, Fe, Co, Cu, Zn, Sn, Ba, Pb
11H (brown-green, uncleaned)	XRF	Ca, Cr, Mn, Fe, Zn, Ba, Pb
12H (brown, cleaned):	XRF	Ca, Cr, Fe, Cu, Sn, Ba, Pb
13H (white, cleaned):	XRF	Ca, Cr, Mn, Fe, Cu, Zn, Sn, Ba, Pb
14H (blue, cleaned):	XRF	Ca, Fe, Cu, Sn, Pb
15H (brown, cleaned):	XRF	Ca, Cr, Fe, Cu, Zn, Sn, Ba, Pb
16H (white, cleaned):	XRF	Ca Cr, Mn, Fe, Cu, Zn, Sn, Ba, Pb
17H (blue, cleaned):	XRF	Ca, Fe, Cu, Sn, Pb
18H (blue, cleaned):	XRF	Ca, Cr, Fe, Cu, Zn, Ba, Pb
19R (whitish, cleaned)	Raman Spectroscopy	Calcite
20R (blue, uncleaned)	Raman Spectroscopy	Lead white, Ultramarine blue
21R (blue, cleaned)	Raman Spectroscopy	Lead white, Anatase; Micro-SORS sequence: lead white under titanium white
22R(whitewash, cleaned)	Raman Spectroscopy	Calcite, Gypsum
23R (brown, cleaned)	Raman Spectroscopy	Calcite
24R (blue, uncleaned)	Raman Spectroscopy	Calcite, Ultramarine blue, Baryte
25R (blue, uncleaned)	Raman Spectroscopy	Ultramarine blue, Gypsum
26R (lacuna of the external paint layer(s), uncleaned)	Raman Spectroscopy	Calcite, Lead white, (Ultramarine blue traces)
27R (blue, uncleaned)	Raman Spectroscopy	Calcite, Ultramarine blue, Quartz
28R (blue, cleaned)	Raman Spectroscopy	Ultramarine blue
29R (green, cleaned)	Raman Spectroscopy	Calcite
30R (white, cleaned)	Raman Spectroscopy	Calcite
31R (blue, cleaned)	Raman Spectroscopy	Calcite, Lead white,
32R (blue, uncleaned)	Raman Spectroscopy	Ultramarine blue
33R (brown, uncleaned)	Raman Spectroscopy	Calcite
34R (blue, cleaned)	Raman Spectroscopy	Calcite, Lead white
35R (blue, cleaned)	Raman Spectroscopy	Ultramarine blue, Gypsum
36R (blue, uncleaned)	Raman Spectroscopy	Calcite, Ultramarine blue, Gypsum, Baryte

In line with expectations, point XRF elemental analyses confirmed the results obtained with XRF mapping; in particular, zinc, barium, manganese and chrome are more abundant in the uncleaned sides, although they have been detected in almost each analysed point, including the cleaned areas. One of the key findings is the detection of tin traces across most measurement points, observed on both the cleaned and uncleaned areas. Additionally in the uncleaned parts, cobalt was identified in a blue area (Table 1, measurements 10H) (Fig. 7c, d), and antimony traces were identified in a green uncleaned area (Table 1, measurement 1H) (Fig. 7a, b).

In the blue areas of the cleaned portions the detected chromophore element is copper, indicating the presence of a copper-based blue pigment. This is most probably azurite, that is the most used copper-based blue pigment in European paintings during all the Middle Ages, until the end of 15th century and later [26]. The presence of azurite was not confirmed by Raman spectroscopy measurements, probably because of its relatively low Raman scattering cross-section.

In the cleaned blue areas, instead, lead white, calcite, gypsum and ultramarine blue were identified with Raman spectroscopy. Ultramarine blue was also detected in all point measurements acquired on uncleaned blue areas, alone or with other compounds as calcite, gypsum, baryte and lead white.

The interpretation of these data has to be done considering the fact that in the 15th century, only natural ultramarine was available, and due to its high cost, it was rarely used for large surfaces. However, by the time the overpaintings were applied, synthetic ultramarine—an inexpensive alternative—was widely accessible. Therefore, the presence of ultramarine blue in the cleaned part is likely a remnant of the overpainting that was not entirely removed during the cleaning process. As supporting evidence for this interpretation, no luminescence bands were observed in the spectra of ultramarine blue (Fig. 8a). Raman spectra of natural ultramarine blue acquired with a 785 nm laser often show a strong luminescence signature between 1200 and 2000 cm^{-1} [27,28]. However, in the spectra collected in the Sala, this region is dominated only by spectral artifacts, which appear in all spectra regardless of the analysed pigments. For comparison, a spectrum with artefacts from a white, cleaned area is also shown in Fig 8a.

Micro-SORS conducted on the light blue part of the cleaned area shed light on its stratigraphy, showing that anatase, one of the titanium dioxide mineralogical phases, is spread on top of lead white (Table 1, measurement 21R). Fig. 8b shows the evolution of the micro-SORS sequence. The increase in lead white signal from the subsurface revealed the presence of a more ancient layer over which a titanium white layer, a pigment introduced in the twentieth century, has been applied. This confirms a multifaceted scenario where modern and ancient layers still coexist, even in the cleaned areas. The presence of lead white in a lacuna of the more recent paint (Table 1, measurement 26R) confirmed this stratigraphy.

Point Raman measurements in the spectra collected on the whitish areas highlight the vibrational pattern of calcite, possibly arising from the plaster. In one spectrum collected on a whitewash relic in the CT1 (Table 1, measurements 22R), a significant amount of gypsum is also present together with calcite.

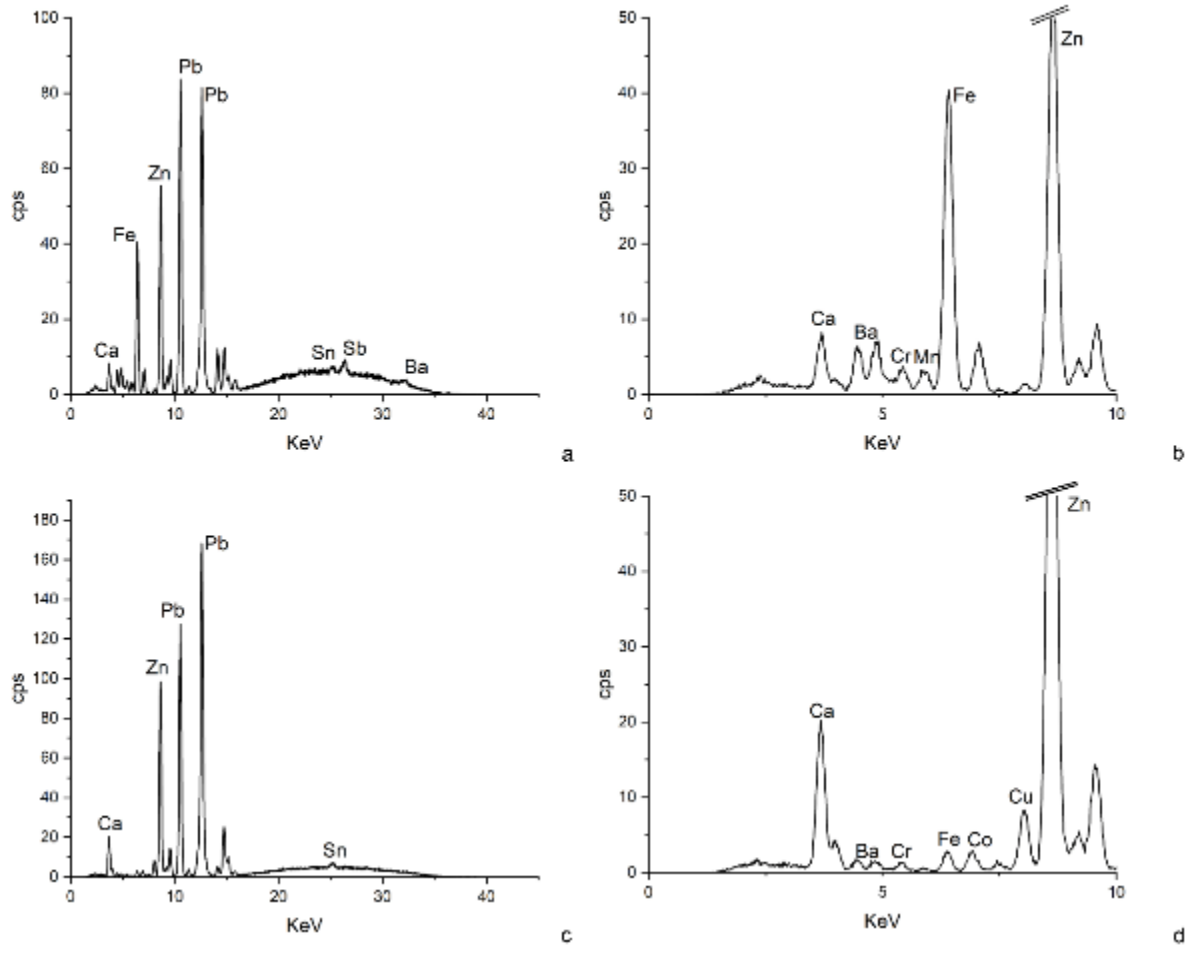

Fig. 7. Point XRF measurements: (a) H1, 0-50 KeV region; (b) H1, 0-10 KeV region; (c) H10, 0-50 KeV region; (d) H10, 0-10 KeV region.

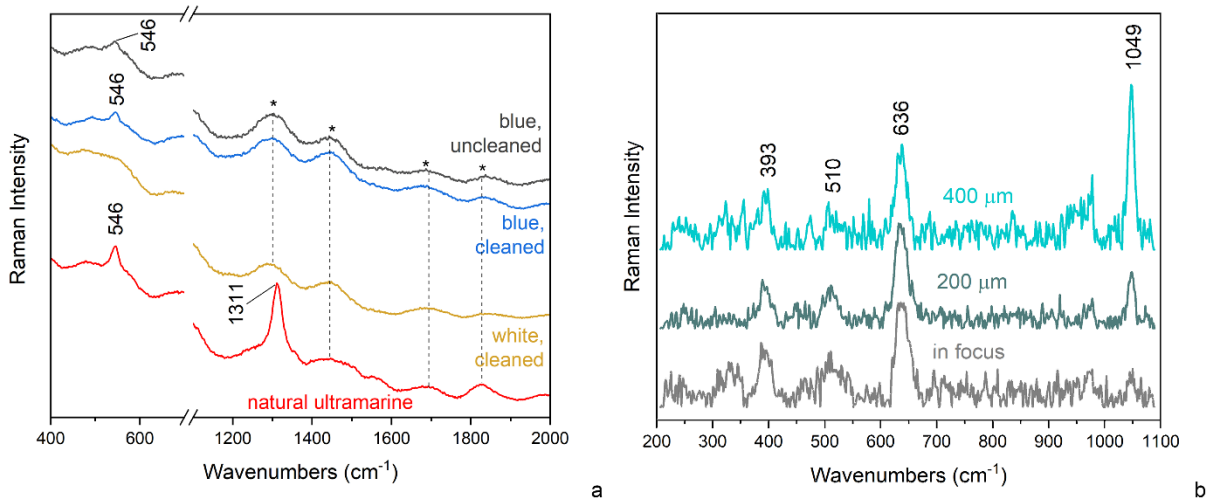

Fig. 8. a) Raman spectra collected with portable Xantus-2™ Raman spectrometer on blue areas (20R, uncleaned and 35R, cleaned), white area (30R, cleaned) and on a blue area of an illuminated manuscript [29] where natural ultramarine blue was identified. Spectral artefacts are indicated with (a). Micro-SORS sequence acquired on a whitish area of cleaning test CT1 (21R). The presence of lead white (1049 cm^{-1}) under titanium white (636, 510, 593 cm^{-1}) is inferred by the relative increase of the lead white Raman band with the increase of the defocusing distance.*

The clustering procedure provides the mean cluster spectra, that can be used to identify the materials present on the surface of the painting. Nonetheless, the interpretation of these spectra can be challenging especially in complex situations such as those observed in the *Sala*. For a more accurate interpretation of reflectance spectra, the combination of data acquired with Raman spectroscopy and XRF is found to be essential: the average cluster reflectance spectra were fitted using selected pigment mixtures based on the results obtained from XRF mapping, XRF point measurements, and Raman spectroscopy. The average reflectance spectrum of the main cluster on the blue sky region of the uncleaned portion of the wall was well fitted using Kubelka-Munk (KM) model using as a reference ultramarine blue, that was identified with Raman spectroscopy measurements, and a white component [30,31]. Several attempts were made to fit the reflectance mean spectrum of the cluster that corresponds to the uncleaned tree and foliage using different pigment mixtures based on suggestions provided by XRF mappings and XRF point analyses; the best fit KM was achieved using as references viridian green (hydrated chromium (III) oxide), ochre and a white component (Fig. 9)[30,31]. The advantage of this protocol is that once the relation between point analyses and reflectance mean cluster spectra is established, the findings can be extended to a large portion of the wall, following the distribution of the clusters; one of the most interesting results is that viridian and ultramarine blue clusters are present, even if less abundantly, also in the cleaned portion of the wall, confirming the presence of modern paint residues in the cleaning test areas.

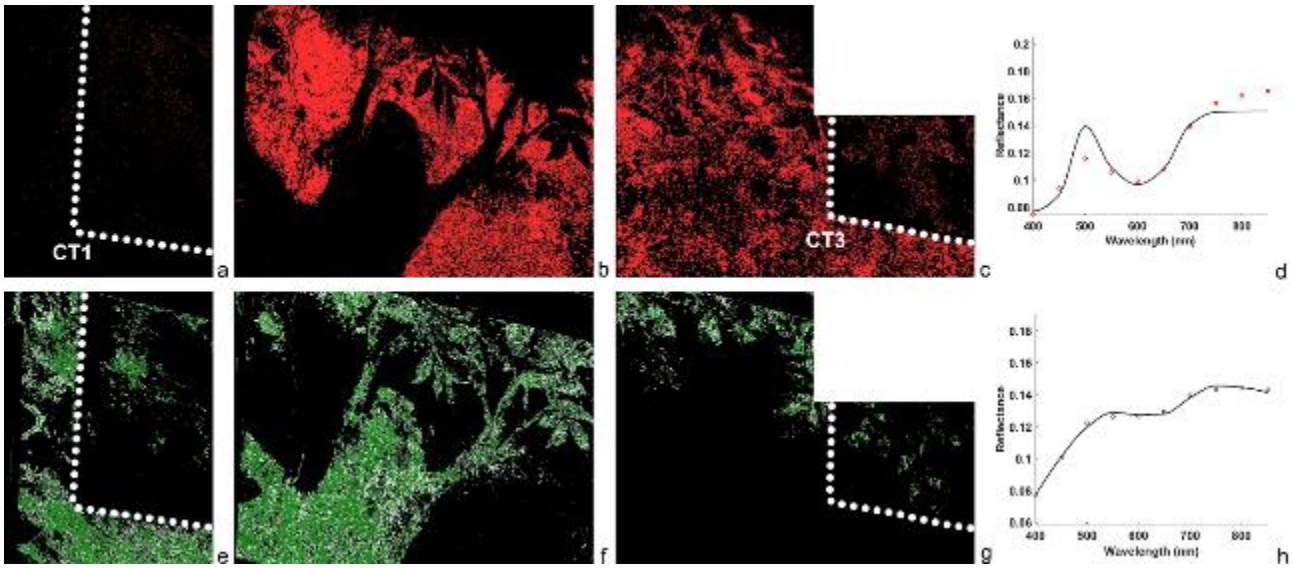

Fig. 9. Cluster maps that correspond to an uncleaned portion of the sky (a-c) along with the associated mean reflectance spectrum, fitted with ultramarine blue and a white component using Kubelka-Munk (KM) model (d); cluster maps corresponding to a tree and its leaves (e-g) along with the associated mean reflectance spectrum, fitted with viridian green, ochre and Zn-containing white using KM model (h). Cleaning tests CT1 and CT3 (dotted lines) are indicated in a, c, e and g. The reflectance spectra were fitted using the method described by Liang et al.[30,31] Overall cluster maps of the same area are visible in Fig. 3.

3.1 Layer sequence reconstruction

Based on the results achieved by the multimodal and multiscale protocol the reconstruction of the stratigraphy of the wall can be inferred as follows:

1) Ancient paint layers: blue areas are made of lead white and a copper-based blue, most probably azurite; in the green and brown areas, copper-based green pigments (malachite, verdigris or copper resinate) are possibly present, together with a lead-containing pigment. The trace of tin in the XRF spectra suggests the presence of lead tin yellow; due to its widespread detection, the pigment may also have been used in a ground layer above the plaster. The present results have been compared with the literature findings related to the Leonardo's technique. The use of a ground layer, in order to prepare the mural substrate to receive the painting materials, seems part of Leonardo *modus operandi*, since a thin layer of ground lead white was found in cross section samples from the *Last Supper* [4–6].

2) Whitewash: in the residues of the layers used to cover the 15th century painting, calcite-based remnants have been detected, with presence of gypsum possibly derived from sulphation of calcite.

3) In the 19th-20th century layers, blue areas of ultramarine blue, green and brown areas of ochres and viridian green have been highlighted. These pigments were mixed with zinc containing compounds, such as zinc white, and baryte. Also the presence of lithopone cannot be excluded. Lead and copper containing pigments are possibly present as well as an antimony-containing compound such as Naples yellow and a cobalt-based pigment such as cobalt blue. Titanium white was also found over the 15th layers. Residues of 19th-20th century layers have been identified in the cleaned areas.

4. CONCLUSIONS

This study highlights the effective combination of several non-invasive and complementary analysis to identify pigments used for the ancient painting and the 19th-20th centuries restorations, and to achieve relevant information about the result of the cleaning procedure. The remote reflectance spectral imaging permitted the analysis of large painted areas at high resolution at difficult to access areas. Detailed painting

materials identification was performed on accessible regions of the walls with XRF maps, Raman spectroscopy and XRF point measurements. The analytical protocol was developed with the aim of achieving complementary information: VIS-NIR reflectance mean cluster spectra guided the XRF and Raman measurements and, at the same time, XRF and Raman measurements permitted to properly interpret VIS-NIR reflectance spectra. The point analysis and micro-mapping provided information of both surface and subsurface so that a paint layer sequence could be hypothesized.

The combined use of Raman spectroscopy and XRF micro-mapping and reflectance spectral imaging showed interesting potentials, that expand the up-to-date protocols for the non-invasive identification of pigments and for evaluating the presence of unwanted residues after the cleaning of painted surfaces. The analytical protocol adopted could be part of an integrated evaluation of cleaning effectiveness, especially in those cases where the distribution of chemical elements characterizes differently the uncleaned part from the cleaned one. The case of murals with large overpainting is a perfect example of this kind of application.

Recently the technical committee of the European Standardization body - CEN TC 346 Conservation of Cultural Heritage - published a document concerning the test methodology for the evaluation of both harmfulness and effectiveness of a cleaning method, as applied to porous inorganic materials[32] . Mural paintings and polychromy are not considered by this document, mainly because of their intrinsic compositional complexity. The study presented here can be a first contribute to broaden the aims of the European document.

5. ACKNOWLEDGMENTS

"Non-invasive micro-scale depth resolved imaging and sensing of materials in cultural heritage", International Exchanges 2020 Cost Share (Italy), funded by the Royal Society (2021-2023).

6. DECLARATION OF INTEREST:

None.

7. REFERENCES

[1] Palazzo M. I restauri dei dipinti murali della Sala delle Asse e delle sale terrene della Corte Ducale nel Castello Sforzesco di Milano. Politecnico di Milano, 2017.

[2] Tasso F. La camera granda da le Asse coè da la tore, from Galeazzo Maria Sforza to Luca Beltrami. In: Tasso F, Palazzo M, editors. Leonardo da Vinci. The Sala delle Asse of the Sforza Castle – Diagnostic Testing and Restoration of the Monochrome. Silvana Editoriale, 2017, p. 26–55.

[3] Gonzalez V, Hageraats S, Wallez G, Eveno M, Ravaud E, Réfrégiers M, et al. Microchemical analysis of Leonardo da Vinci's lead white paints reveals knowledge and control over pigment scattering properties. Sci Rep 2020;10. https://doi.org/10.1038/s41598-020-78623-5.

[4] Osticioli I, Pagliai M, Comelli D, Schettino V, Nevin A. Red lakes from Leonardo's Last Supper and other Old Master Paintings: Micro-Raman spectroscopy of anthraquinone pigments in paint cross-sections. Spectrochim Acta A Mol Biomol Spectrosc 2019;222. https://doi.org/10.1016/j.saa.2019.117273.

[5] Newton HT. Leonardo da Vinci as mural painter: some observations on his materials and working methods. In: Basile G, Marabelli M, editors. Leonardo. L'Ultima Cena. Indagini, ricerche, restauro. Nardini Editore, Firenze: 2007, p. 116–25.

[6] Matteini M, Moles A. A preliminary investigation of the unusual technique of Leonardo's mural The Last Supper. In: Basile G, Marabelli M, editors. Leonardo. L'Ultima Cena. Indagini, ricerche, restauro. Nardini Editore, Firenze: 2007.

[7] De Viguerie L, Walter P, Laval E, Mottin B, Solé VA. Revealing the sfumato technique of leonardo da vinci by X-ray fluorescence spectroscopy. Angewandte Chemie - International Edition 2010;49:6125–8. https://doi.org/10.1002/anie.201001116.

[8] Gonzalez V, Wallez G, Ravaud E, Eveno M, Fazlic I, Fabris T, et al. X-ray and Infrared Microanalyses of Mona Lisa's Ground Layer and Significance Regarding Leonardo da Vinci's Palette. J Am Chem Soc 2023;145:23205–13. https://doi.org/10.1021/jacs.3c07000.

[9] Menu M, editor. Leonardo da Vinci's technical practice: Paintings, drawings and influence . Paris: Hermann; 2014.

[10] Newton HT. Leonardo Da Vinci as Mural Painter: Some Observations on His Materials and Working Methods. ARTE LOMBARDA 1983;66:71–88.

[11] Keith L, Ashok R, Morrison R, Schade P. E KEITH, L., ROY, A., MORRISON, R., & SCHADE, P. (2011). Leonardo da Vinci's "Virgin of the Rocks": Treatment, Technique and Display. National Gallery Technical Bulletin 2011;32:32–56.

[12] Cucci C, Picollo M, Chiarantini L, Uda G, Fiori L, De Nigris B, et al. Remote-sensing hyperspectral imaging for applications in archaeological areas: Non-invasive investigations on wall paintings and on mural inscriptions in the Pompeii site. Microchemical Journal 2020;158. https://doi.org/10.1016/j.microc.2020.105082.

[13] Cano N, de Lucio OG, Pérez M, Mitrani A, Nagaya A, Sil JLR, et al. Acrylic colors for peace: Non-invasive study of an outdoor mural painting. Color Res Appl 2023;48:381–92. https://doi.org/10.1002/col.22861.

[14] Andreotti A, Izzo FC, Bonaduce I. Archaeometric Study of the Mural Paintings by Saturnino Gatti and Workshop in the Church of San Panfilo, Tornimparte (AQ): The Study of Organic Materials in Original and Restored Areas. Applied Sciences 2023;13. https://doi.org/10.3390/app13127153.

[15] Menegaldo B, Aleccia D, Nuyts G, Amato A, Orsega EF, Moro G, et al. Stories of the Life of Saint George: Materials and Techniques from a Barbelli Mural Painting. Studies in Conservation 2023. https://doi.org/10.1080/00393630.2023.2262842.

[16] Gay M, Plassard F, Müller K, Reiche I. Relative chronology of Palaeolithic drawings of the Great Ceiling, Rouffignac cave, by chemical, stylistic and superimposition studies. J Archaeol Sci Rep 2020;29. https://doi.org/10.1016/j.jasrep.2019.102006.

[17] May SK, Huntley J, Marshall M, Miller E, Hayward JA, Jalandoni A, et al. New Insights into the Rock Art of Anbangbang Gallery, Kakadu National Park. J Field Archaeol 2020;45:120–34. https://doi.org/10.1080/00934690.2019.1698883.

[18] Rousaki A, Vandenabeele P, Berzioli M, Saccani I, Fornasini L, Bersani D. An in-and-out-the-lab Raman spectroscopy study on street art murals from Reggio Emilia in Italy. Eur Phys J Plus 2022;137. https://doi.org/10.1140/epjp/s13360-022-02423-1.

[19] Brunetti B, Miliani C, Rosi F, Doherty B, Monico L, Romani A, et al. Non-invasive investigations of paintings by portable instrumentation: The MOLAB experience. Top Curr Chem 2016;374:1–35. https://doi.org/10.1007/s41061-015-0008-9.

[20] Liang H, Lucian A, Lange R, Cheung C, Su B. Remote spectral imaging with simultaneous extraction of 3D topography for historical wall paintings. ISPRS Journal of Photogrammetry and Remote Sensing 2014;95:13–22. https://doi.org/10.1016/j.isprsjprs.2014.05.011.

[21] Kogou S, Shahtahmassebi G, Lucian A, Liang H, Shui B, Zhang W, et al. From remote sensing and machine learning to the history of the Silk Road: large scale material identification on wall paintings. Sci Rep 2020;10. https://doi.org/10.1038/s41598-020-76457-9.

[22] Li Y, Cheung CS, Kogou S, Hogg A, Liang H, Evans S. ICOM-CC 19th Triennial Conference Standoff laser spectroscopy for wall paintings, monuments and architectural interiors. n.d.

[23] Li Y, Cheung CS, Kogou S, Liggins F, Liang H. Standoff Raman spectroscopy for architectural interiors from 3-15 m distances. Opt Express 2019;27:31338. https://doi.org/10.1364/oe.27.031338.

[24] Botteon A, Colombo C, Realini M, Castiglioni C, Piccirillo A, Matousek P, et al. Non-invasive and in situ investigation of layers sequence in panel paintings by portable micro-spatially offset Raman spectroscopy. Journal of Raman Spectroscopy 2020;51:2016–21. https://doi.org/10.1002/jrs.5939.

[25] Mosca S, Conti C, Stone N, Matousek P. Spatially offset Raman spectroscopy. Nature Reviews Methods Primers 2021;1:22. https://doi.org/10.1038/s43586-021-00019-0.

[26] Roy A, editor. Artists' Pigments. A Handbook of Their History and Characteristics. vol. Volume 2. London: Archetype Publications; 1993.

[27] González-Cabrera M, Arjonilla P, Domínguez-Vidal A, Ayora-Cañada MJ. Natural or synthetic? Simultaneous Raman/luminescence hyperspectral microimaging for the fast distinction of ultramarine pigments. Dyes and Pigments 2020;178. https://doi.org/10.1016/j.dyepig.2020.108349.

[28] Schmidt CM, Walton MS, Trentelman K. Characterization of lapis lazuli pigments using a multitechnique analytical approach: Implications for identification and geological provenancing. Anal Chem 2009;81:8513–8. https://doi.org/10.1021/ac901436g.

[29] Pietroni E, Botteon A, Buti D, Chirivì A, Colombo C, Conti C, et al. "Codex 4D" Project: Interdisciplinary Investigations on Materials and Colors of De Balneis Puteolanis (Angelica Library, Rome, Ms. 1474). Heritage 2024;7:2755–91. https://doi.org/10.3390/heritage7060131.

[30] Liang H, Keita K, Peric B, Vajzovic T. Pigment identification with optical coherence tomography and multispectral imaging. Proc. OSAV'2008, The 2nd Int. Topical Meeting on Optical Sensing and Artificial Vision, 2008, p. 33–42.

[31] Liang H. Advances in multispectral and hyperspectral imaging for archaeology and art conservation. Appl Phys A Mater Sci Process 2012;106:309–23. https://doi.org/10.1007/s00339-011-6689-1.

[32] EN 17488:2021 - Conservation of cultural heritage - Procedure for the analytical evaluation to select cleaning methods for porous inorganic materials used in cultural heritage n.d.